Progress In Electromagnetics Research B, Vol. 43, 35–52, 2012

BROADBAND MATERIAL CHARACTERIZATION USING TRAVELING-WAVE WHISPERING-GALLERY -MODE DIELECTRIC RESONATORS

M. S. Kheir[1, *], H. F. Hammad[1], and A. Omar[2]

[1]Faculty of Information Engineering and Technology, German University in Cairo, New Cairo, Cairo 11835, Egypt

[2]Chair of Microwave and Communication Engineering, University of Magdeburg, Magdeburg 39106, Germany

Abstract—A new technique for broadband material characterization, using a whispering-gallery-mode (WGM) resonator, is proposed. The resonant perturbation method is applied for the measurement of both the dielectric constant and loss tangent of various types of materials and over a wide frequency band. A comprehensive study on the reliability of using such technique, via simulations and measurements, is conducted as well. The feasibility of this device in sensing small variations of the dielectric properties of the material is investigated. Furthermore, the geometry of the resonator is slightly modified to fit liquid materials as well. This can be a promising solution for sensing human-body tissues or liquids such as blood or urine due to the sensitive nature of these resonators. The experimental setup is successfully utilized to measure the dielectric constant of a water droplet as a liquid sample as well as different material samples of arbitrary shapes and dielectric properties. The measurements are performed over the whole X- and K-bands where the obtained results are with a maximum deviation of only 3.3% for solids and 4.5% for liquids.

1. INTRODUCTION

Material characterization techniques are generally classified as resonant or non-resonant [1–5]. Non-resonant techniques, such as reflection, transmission/reflection or free-space, are non-destructive and broadband [2, 3, 5]. Resonant techniques, such as cavity or ring

Received 5 July 2012, Accepted 6 August 2012, Scheduled 9 August 2012

* Corresponding author: Mohamed S. Kheir (mohamed.salah-kheir@guc.edu.eg).

resonators, are still the most accurate among all techniques though they are typically narrow-band [1, 4, 8].

Whispering-gallery-mode (WGM) resonators are proposed in this paper to account for this problem [6, 7]. They have many advantages over the conventional dielectric resonators especially at mm-wave and THz frequency bands. Some of these advantages are their controllable size, their high Q-factor and their capability of spurious modes suppression. Material characterization using WGM resonators has proven to be efficient, due to their highly sensitive nature, and succeeded to play a great role in characterizing ultra low-loss materials [8–13]. Whispering-gallery modes can be categorized into standing- or traveling-wave modes depending on the coupling mechanism.

Traveling-wave modes can be excited in a resonator placed in the proximity of a traveling-wave source like a microstrip line or a dielectric image guide (DIG) in a reaction-type coupling. This type of coupling occurs when the resonator is coupled to a transmission line in a tangential configuration. At resonance, the power is coupled from the transmission line to the resonator. DIG has been chosen due to the lower amount of conductor losses which significantly increase at higher frequencies. The modes excited in a resonator coupled to a DIG are the so-called $\mathrm{WGE}_{n,m,l}$ (quasi-TE) modes [6]. The subscripts n, m and l denote, respectively, the order of azimuthal, radial and axial dependence. Planar WGM resonators, which have been originally investigated by Cros and Guillon [6] and Jiao et al. [7], are employed in this work due to their compact size and higher field confinement. Such type of modes can be excited in a thin dielectric disk whose diameter is much greater than its height. They are featured by having only azimuthal propagation modes and the resonant frequency does not depend on the height of the disk.

The concept of using such resonators in material characterization is to measure the frequency shift and Q-factor variation after perturbing the resonator. By measuring these parameters, the dielectric constant and loss tangent, respectively, can be determined. The useful feature in WGM resonators is that they offer multi-mode resonance; which means that the frequency band will be occupied by several equally separated resonances. Measuring material properties at each resonance frequency will result in a broadband material characterization approach. In this paper, WGM resonators have been proposed for characterizing different dielectric materials of any form or shape, liquid or bulk.

A comprehensive study has been conducted in this paper where it was proved that these resonators are insensitive to volume or shape

variations. They are, however, very sensitive to any slight variation in dielectric properties. Therefore, the material under test (MUT) does not need to be machined into a specific geometry before testing like the case of cavity resonators. The MUT here is the dielectric sample to be tested either in solid or liquid form. The resonant perturbation approach has been examined in this paper as well to investigate its efficiency in dealing with open resonators such as WGM resonators for the first time. In addition to that, the main advantage here lies in the simplicity of the measurement prototype. Most of the techniques based on WGM typically suffer from the design and implementation complexity [9, 10].

2. RESONANT PERTURBATION METHOD

Resonant perturbation is a well-known and widely used method for material parameter extraction using microwave resonators [14, 15]. It is mainly used for medium-loss and low-loss material characterization using cavity resonators. However, cavity resonators are typically restricted to relatively low frequencies since they exhibit high conductor losses and their size become impractically small in the higher frequency ranges. The perturbation method extracts the complex relative dielectric constant ($\varepsilon_r^* = \varepsilon_r' - j\varepsilon_r''$) of the MUT based on the fact that the boundary conditions at the cavity walls do not change before or after material inclusion, where ε_r' is the relative dielectric constant and ε_r'' is the loss factor. The proposed WGM resonator is an open structure and the propagation is merely in the azimuthal direction since it is a planar WGM resonator. Therefore, the normal E-field component will be insignificant here and will not violate the theory. The complex angular frequency change is represented as [14]

$$\frac{\omega_2 - \omega_1}{\omega_2} = -\left(\frac{\varepsilon_r - 1}{2}\right) \frac{\iiint\limits_{V_S} \underline{E}_1 \cdot \underline{E}_2 \, dV}{\iiint\limits_{V_C} |\underline{E}_1|^2 \, dV} \tag{1}$$

where ω_1 and ω_2 are the angular frequencies after and before sample perturbation, respectively. E_1 and E_2 represent the electric field intensity before and after sample perturbation, respectively.

It is assumed that the MUT is homogenous and non-magnetic. The negative sign in (1) indicates that the frequency lowers due to sample perturbation.

The previous equation can be expanded into two separate equations, real and imaginary parts, according to

$$\frac{\omega_2 - \omega_1}{\omega_2} = \left(\frac{f_2 - f_1}{f_2}\right) + j\left(\frac{1}{2Q_2} - \frac{1}{2Q_1}\right) \tag{2}$$

Therefore, (1) can be expressed as

$$2\left(\frac{f_1 - f_2}{f_2}\right) = \left(\varepsilon_r' - 1\right)\ C \tag{3a}$$

and

$$\frac{1}{Q_2} - \frac{1}{Q_1} = C\varepsilon_r'' \tag{3b}$$

with

$$C = \frac{\iiint\limits_{V_S} \underline{E}_1 \cdot \underline{E}_2\, dV}{\iiint\limits_{V_C} \left|\underline{E}_1\right|^2 dV} \tag{4}$$

where f_1, f_2, Q_1 and Q_2 are the resonance frequencies and unloaded quality factors measured before and after material perturbation, respectively. The term dV represents the differential element for the volumetric integral.

C is assumed to be a constant independent of the material properties of the sample which is difficult to evaluate analytically. Therefore, two alternative parameters, A and B are proposed instead of C, which simplifies the material extraction process. These parameters are related to the configuration and field distribution of the resonator. They can be directly evaluated by a calibration procedure with a material of known ε_r' and ε_r'' [14]. Now (3a) and (3b) will be rewritten as

$$\frac{f_1 - f_2}{f_2} = A\left(\varepsilon_r' - 1\right)\ \frac{V_S}{V_C} \tag{5a}$$

$$\frac{1}{Q_2} - \frac{1}{Q_1} = B\ \varepsilon_r''\ \frac{V_S}{V_C} \tag{5b}$$

where V_c and V_s represent the volume of the cavity and the volume of the sample, respectively. Before running the perturbation experiment, a careful study on the validity of this method with WGM resonators was conducted. Equations (5a) and (5b) are based on some assumptions and restrictions that should be maintained in order to obtain reliable results [14, 15]. One of the most fundamental assumptions is that the fields inside the resonator should not be considerably influenced due to the introduction of the MUT. The perturbation theory assumes that the fields on the MUT are uniform over its volume, which is also satisfied here.

In order to validate this assumption, some full-wave simulations using CST Microwave Studio [19] have been performed to observe the E-field distribution before and after sample intrusion. In this

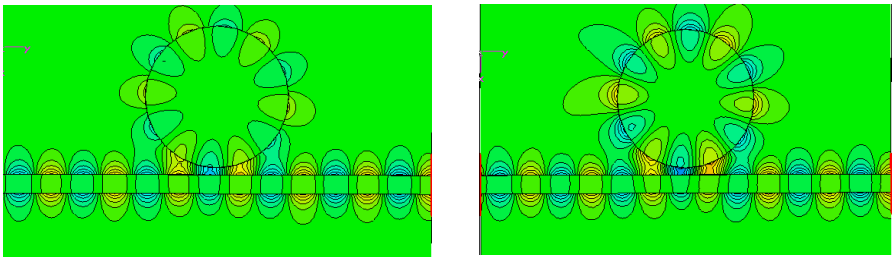

(a) (b)

Figure 1. E-field distribution of the $WGE_{12,0,0}$ mode within the resonator (a) before and (b) after material perturbation.

simulation, a WGM resonator is used with a relative dielectric constant of 10 and loss tangent of 0 perturbed by a material with a dielectric constant of 4 and a loss tangent of 0.002. The resulted field distributions in both cases are shown in Fig. 1.

Figure 1(a) shows the resonator coupled to the DIG at a certain frequency. The same figure indicates that the mode excited at this frequency is $WGE_{12,0,0}$. Fig. 1(b) shows the same resonator after the MUT has been placed on top of it. The MUT is of a disk shape as well and totally covers the disk resonator with a volume 20% of the resonator volume. The same field distribution can be clearly noticed at the same frequency. The contour lines of both figures indicate that the E-field intensity has been increased due to material perturbation. This indicates that the sensitivity of the resonator to any external perturbation is relatively high.

The second assumption states that the difference between the cavity wall losses before and after perturbation is negligible. In our case, there is only one metallic wall which is the ground plane. This ground plane does not exhibit significant losses due to the fact that the electric fields of the planar WGM resonator move essentially against the concave side of the disk resonator.

The third assumption states that Q_1 and Q_2 are measured at the same frequency and the coupling conditions of the resonator to the external circuit are maintained. To meet this assumption, a groove in the ground plane underneath the resonator and the DIG is etched with a 0.2 mm depth to ensure that the coupling distance is always fixed. It is well-known that the coupling distance significantly affects the Q-factor of the resonator. Therefore, this distance has been optimized by the simulator for the maximum achievable Q.

3. MEASUREMENT OF MATERIAL PARAMETERS

The dielectric material used in fabricating both the image guide and the disk resonator is Alumina with a relative dielectric constant of 9.2 and a loss tangent of 9×10^{-5}. The radius of the K-band resonator is 8 mm with a 2 mm height. The WGM resonator is coupled to a DIG which is connected to two rectangular-to-SMA transitions as shown in Fig. 2. The image guide is inserted inside the waveguide with linearly tapered ends of $5\lambda g$ length, where λg is the guided wavelength. Both the resonator and the image guide are placed on an aluminum ground plane with 2 mm thickness and 0.2 mm deep grooves to maintain a constant coupling as mentioned earlier. The measurements have been performed using an HP-8722D vector network analyzer.

3.1. Dielectric Constant

The corresponding modes for the K-band resonator used in this experiment are $\mathrm{WGE}_{9,0,0}$ up to $\mathrm{WGE}_{13,0,0}$ from 16 GHz to 26 GHz as depicted in Fig. 3. The resonator has been first calibrated by a material, whose dielectric constant is predetermined using a standard waveguide method, to obtain the calibration parameter A. It should be noted that A has to be evaluated at each resonance mode all over the band to obtain reliable results. It is also worth mentioning that the whispering-gallery modes are always equally spaced by a fixed passband. This passband mainly depends on the dielectric constant and the radius of the resonator. This band, however, facilitates observing the resonance frequency shift due to material perturbation as shown in the same figure.

The MUT used in this measurement is polyvinyl chloride (PVC)

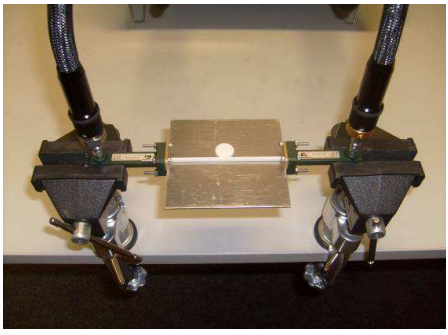

Figure 2. Photograph of the experimental prototype connected to the network analyzer by a pair of waveguide-to-SMA launchers.

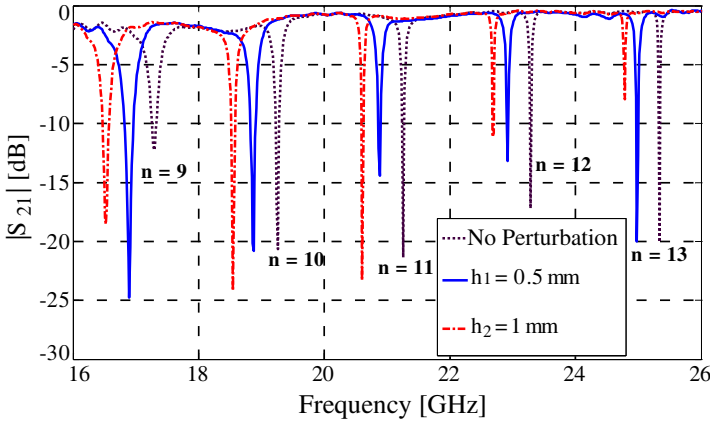

Figure 3. Measured $|S_{21}|$ of the K-band resonator before and after material perturbation.

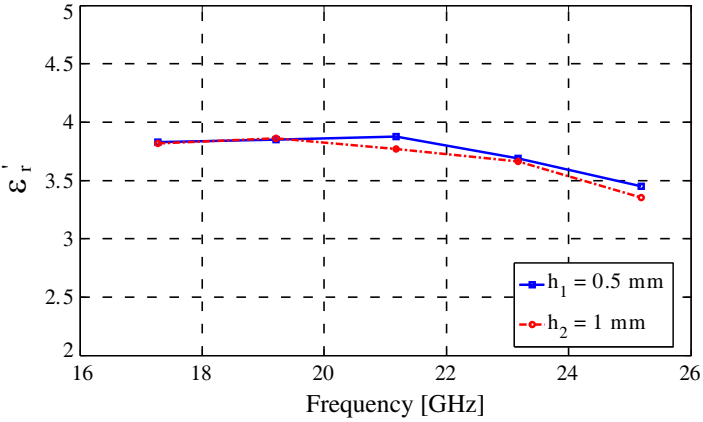

Figure 4. Measured ε'_r from measurements of one material with two different heights h_1 and h_2.

with a dielectric constant of 3.9 [20] machined as a disk with the same radius of the resonator to fully cover it in order to obtain the highest sensitivity. The sample has been prepared into two different heights ($h_1 = 0.5\,\text{mm}$ and $h_2 = 1\,\text{mm}$). The reason of making two different volumes is to verify the extracted values in both cases.

Figure 4 shows that the measured values of ε'_r at each resonance mode for both samples are close and consistent all over the K-band. The value of dielectric constant is almost constant up to around 21 GHz and it drops to 3.5 at 25 GHz which is typical for a dispersive

material. It is worth mentioning that the losses within the MUT increase as frequency increases which is due to dipolar relaxation. This phenomenon has been carefully investigated in [22]. A small deviation of just 0.128 can be observed compared to the standard values [20]. This corresponds to a percentage of only 3.3%. However, such results are reliable and justify the validity of using the perturbation method over a wide frequency range and with open structures such as dielectric resonators.

3.2. Loss Tangent

CST Microwave Studio has been used at first to evaluate the unloaded quality factor, Q_0, of a resonator loaded with two different materials having different values of $\tan\delta$ for verification. Q_0 has been calculated using Microwave Studio according to the fundamental definition shown below [19].

$$Q_0 = \omega_0 \frac{W}{P} \tag{6}$$

where ω_0 is the angular resonance frequency and W the total energy stored in the structure due to electric or magnetic field. At resonance the electric energy stored will be equal to the magnetic energy; hence $W = W_E = W_M$.

$$W_E = \frac{1}{2}\varepsilon_0\,\varepsilon_r \iiint\limits_V |E|^2\, dV \tag{7}$$

P is the average power loss and is given by

$$P = \frac{\omega_0}{2}\tan\delta\,\varepsilon_0\,\varepsilon_r' \iiint\limits_V |E|^2\, dV \tag{8}$$

Except for the electric field intensity E, all other parameters in the above equations are intrinsic parameters and are predefined in the simulator. The peak value of E is typically calculated by a field calculator at the resonance frequency. The values of Q_0 for a dielectric resonator with a relative dielectric constant of 10 and 9×10^{-5} loss tangent with a 10 mm radius are shown in Fig. 5 against the azimuthal modal index n. The resonator has been perturbed by two different materials having the same ε_r' with $\tan\delta = 0.001$ and 0.1. The maximum value obtained for Q_0 was in the case of no perturbation where it reached 6000. For the case of high-loss material perturbation, Q_0 did not exceed 399. It can be concluded from the figure that the value of $\tan\delta$ can significantly affect Q_0 of the resonator since the radiation losses are typically negligible after a certain value of

n (typically 10) [6, 7]. This feature makes this type of resonators extremely sensitive to any variation of the loss tangent of the sample properties.

Based on the previously calculated values of Q_0, the loss tangents of both materials have been determined and the results are shown in Fig. 6. It is true that there is still a deviation between the extracted results and the actual results. This deviation can be due to the fact that the unloaded Q factors calculated by the CST simulator using

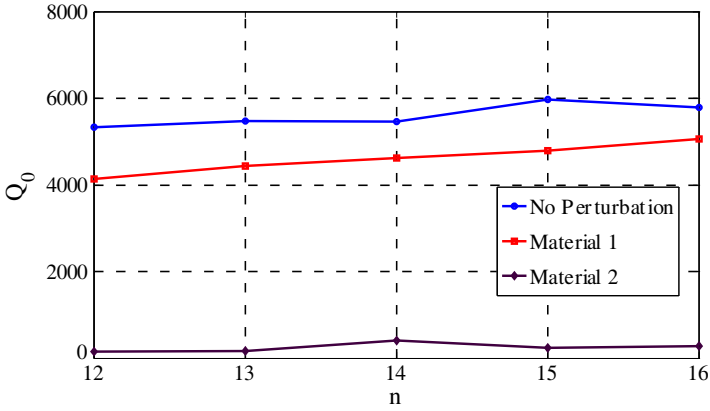

Figure 5. Calculated values of Q_0 of the resonator loaded with two materials having different loss tangents.

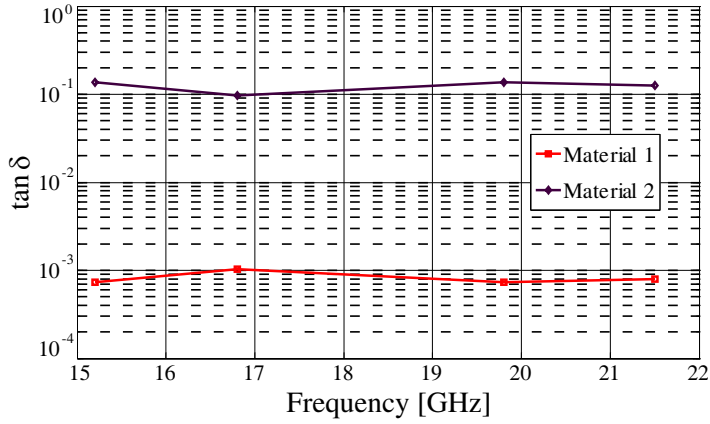

Figure 6. Extracted loss tangent values of both materials. The preset values of materials 1 and 2 are 0.001 and 0.1, respectively.

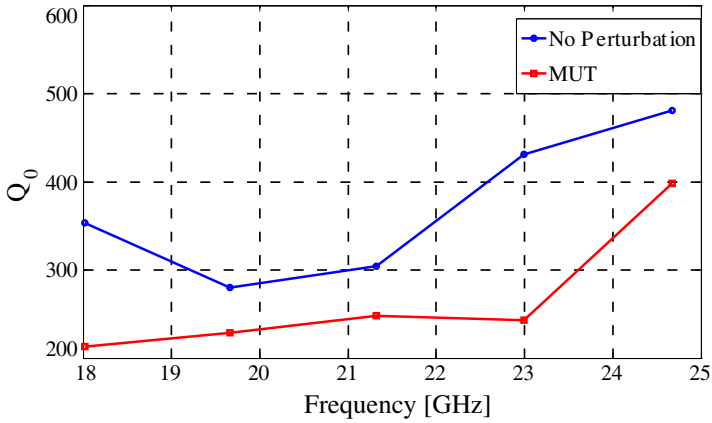

Figure 7. Measured values of Q_0 before and after perturbation.

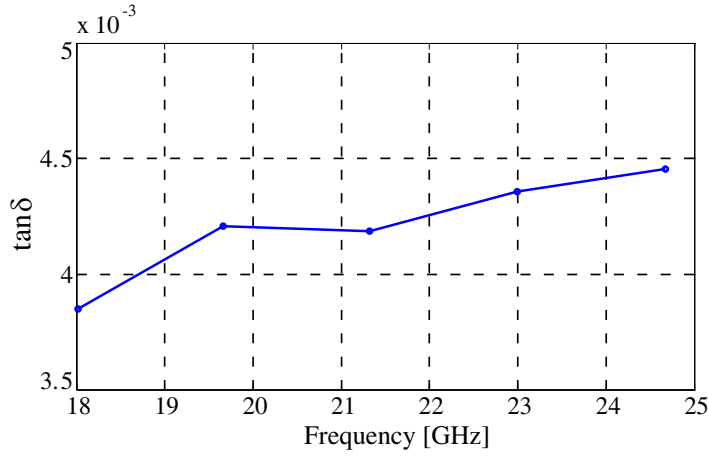

Figure 8. Extracted values of $\tan\delta$ of the MUT obtained by Q-factor measurements.

Equations (6), (7) and (8) are essentially based on the E-field monitor which is strongly frequency-dependent. For our case, this E-filed has been calculated at 16.8 GHz at which it is clear that both extracted values are exactly 0.001 and 0.1. Elsewhere the values are deviated by a percentage of max. 20%.

For the measurement of loss tangent, another dielectric resonator has been employed. It has been fabricated from a ceramic material called AK-10 which is a compound of ceramic and plastic polymers. It has a dielectric constant of 10 and the loss tangent of 0.002 at 10 GHz

according to the vendor data [21]. The radius of this resonator is 10 mm with a height of 3 mm. The reason of utilizing another material for loss tangent measurements is that it has a higher amount of losses. In fact, through our repetitive measurements it has been observed that using a material with some losses provides more reliable results for $\tan\delta$. This resonator has been perturbed by another PVC sample in a disk shape with the same dimensions.

The reaction-type method [16, 17] has been employed for calculating the coupling coefficient to the resonator based on the magnitude of the transmission coefficient $|S_{21}|$. Q_0 values have been obtained for the resonator before and after perturbation as shown in Fig. 7. Based on the calculated values of Q_0, the loss tangent has been extracted and is shown in Fig. 8. The values of $\tan\delta$ vary between 0.0038 and 0.0045 which shows a reasonable agreement with the results published in [3] since losses typically increase with frequency. The $\tan\delta$ value is 0.0033 measured at 2.35 GHz. The maximum value of loss tangent that can be extracted using this method is 0.1. Otherwise the ambiguity in measuring Q-factor would increase. As long as the resonator used for measurement has much lower loss tangent than the MUT, the perturbation approach is still maintained.

3.3. Liquid Materials

Another AK-10 resonator has been fabricated with a 10 mm radius for testing liquid materials. These modifications include making a small hole at the resonator border away from the so-called modal caustic circle [7]. The hole is of a cylindrical shape with a radius and height of 2 mm each which gives a volume of 25.12 mm^3. Fig. 9 shows a photograph of the resonator with the hole which is also coupled to the DIG. A droplet of water of the same volume of the hole has been carefully injected into this hole. In fact, the hole has to be totally

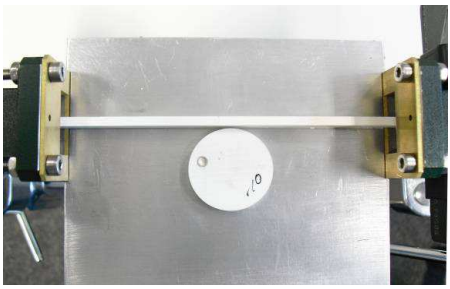

Figure 9. Photograph of the experimental prototype showing the water droplet embedded in the hole

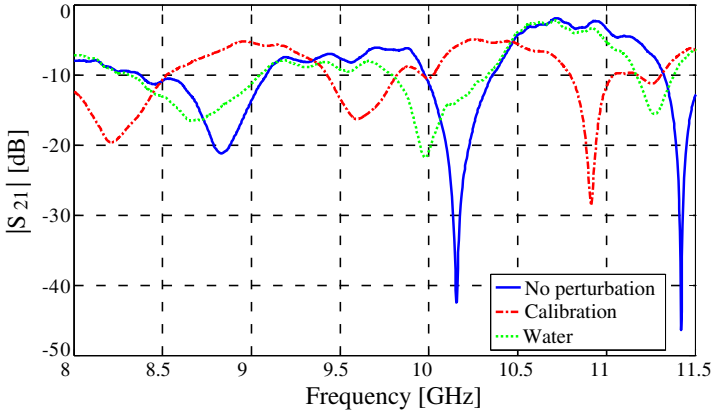

Figure 10. Measured $|S_{21}|$ of the X-band resonator before and after liquid material perturbation.

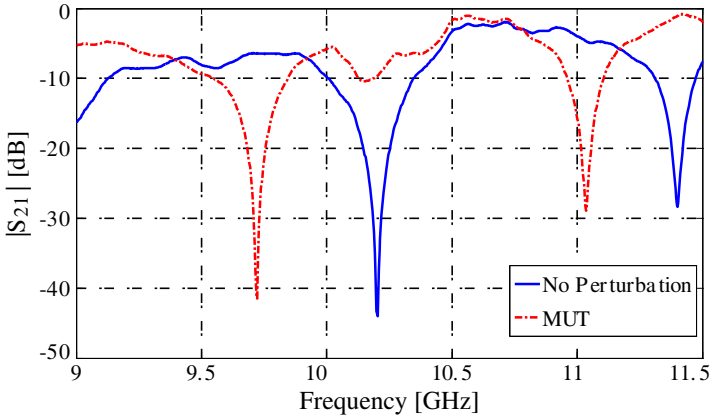

Figure 11. Measured $|S_{21}|$ of the X-band resonator before and after bulk material perturbation.

dry before each experiment. Another important constraint is that the resonator material should be non-absorbing (ceramic, plastic... etc.).

By observing the S_{21} curves, before and after this perturbation, the dielectric properties of this droplet have been obtained as well. The resonator has been first calibrated by a dielectric material of known dielectric constant and loss tangent. This material was in a cylindrical shape with a radius of 10 mm and a height of 3 mm. The material used for calibration was AK-8 with a dielectric constant of 8 and 0.002 loss tangent. Fig. 10 shows the measured S_{21} results at all previous cases. The disk resonator was first loaded by the calibration material

and then by the water droplet. The resulted values of ε'_r of the water droplet at the three resonance modes are 83.33, 76.25 and 77.67 which are quite close to the standard value stated in [18] which is 80. This measurement has been carried out in room temperature. The deviation occurred in this measurement is just 4.5%. The resonator can be also calibrated by another liquid material with known properties which can enhance the accuracy of the measured results.

3.4. Bulk Materials

Another bulk sample of a rectangular-box shape has been tested using the same setup. The material of this sample is Teflon with a dielectric constant of 2.08 at 9 GHz [18]. The volume of this sample is $(22.5 \times 15 \times 10)\,\text{mm}^3$. The measured $|S_{21}|$ of the resonator with and without material perturbation are shown in Fig. 11. The measured values of ε'_r at two successive resonance modes were 2.05 and 2.08. The first value shows a deviation of only 1.4% from the reference value, whereas the second one is exactly the same with no error.

4. SENSITIVITY OF THE RESONATOR

Some preliminary investigations have been performed via simulations and experiments in order to investigate the sensitivity of the resonator. The purpose of these investigations is to check the response of the resonator to any slight variation within the material properties. It was also necessary to investigate its response to the material volume or position and whether it is essential to prepare the samples into certain shape or not. The resonator material used here is also (AK-10). The test sample was fabricated in a disk shape with various dimensions as it will be explained below. Further details can be found in a published article by the authors [22].

4.1. Volume of the Sample

In this study, we have attempted to vary the volume of the material sample according to the values shown in Fig. 12 and observe the results in each case. This figure shows the resulting resonance frequencies against different values of the height of the disk sample. These results have been calculated at the four resonance modes that exist over the X-band for the resonator. These modes are, namely, $\text{WGE}_{9,0,0}$ up to $\text{WGE}_{12,0,0}$. The resonant frequencies of such setup show constant behaviors after a certain value of h which is 3 mm for all modes. The band between all resonance modes is constant, which is another property of all WGM resonators [6].

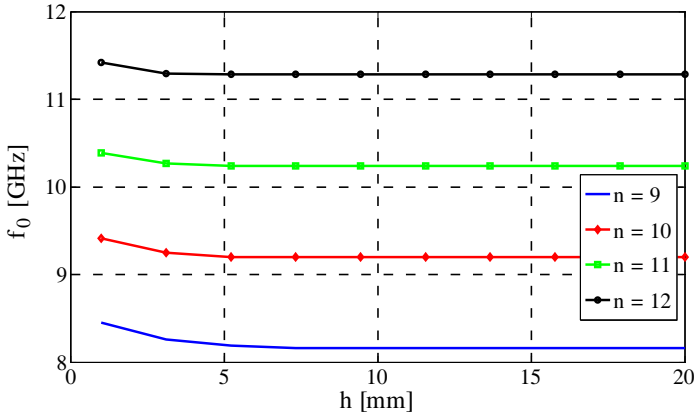

Figure 12. Simulated values of f_0 against the disk height h.

4.2. Position of the Sample

For traveling-wave whispering-gallery modes, it is well-known that they are confined between the outer boundary of the disk and the modal caustic circle and they circulate clockwise or counter clockwise according to the transmission line excitation. The modal caustic circle is a certain area within the WGM resonator at which the field is evanescent [6]. This area is, however, less sensitive than the other part of the resonator and it has to be avoided during measurements in order to have the maximum sensitivity. The disk resonator has been divided into three regions as shown in Fig. 13. The sample has been placed into each region and S_{21} has been measured for each case. The measured results in all positions are almost identical and do not show large deviation between each other. This feature is a property of traveling-wave WG modes, which means that the position of the sample has no influence on the results of measurements. This also applies to the fourth region left on the resonator shown in the same figure.

4.3. Dielectric Constant of the Sample

The same dielectric disk resonator has been employed in the simulator to investigate another property. The disk has been covered by another disk with the same radius with several values of ε'_r varying from 2 up to 10 with a step of only 0.2. The simulated values of the two modes, $WGE_{9,0,0}$ and $WGE_{10,0,0}$, are shown in Fig. 14. Both curves in this figure show different values of f_0 for every single value of ε'_r. This confirms the sensitivity of the resonator to such small variations

within the dielectric constant of the sample. However, the same is also true for all other resonant modes. The calculated sensitivity is 5.6×10^{12} MHz/(Farad/m).

4.4. Loss Tangent of the Sample

The same simulation procedures have been elaborated but with a variable loss tangent material to investigate the response of the resonator to any slight variation within the sample loss tangent. The starting value of $\tan\delta$ in this experiment was 10^{-5} and varied up to 0.01 with a step of 5×10^{-4} as shown in Fig. 15. The loss tangent values are simulated versus the $|S_{21}|$ where the sensitivity of the resonator to this small variation is still high as in the previous case of the dielectric constant for both resonant modes.

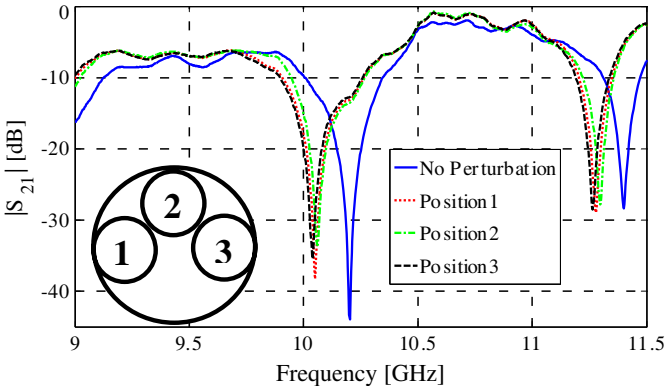

Figure 13. Measured values of $|S_{21}|$ at different positions of the MUT on top of the resonator.

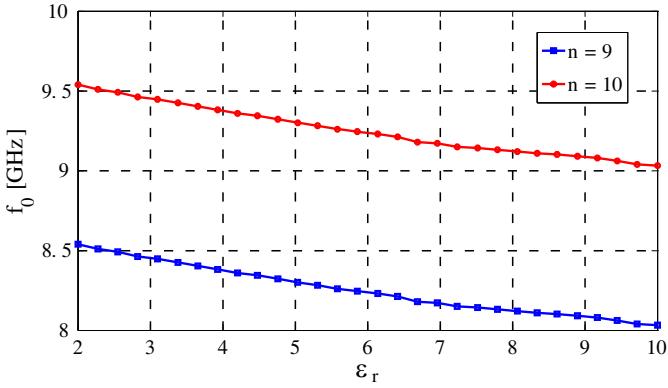

Figure 14. Simulated values of f_0 against different dielectric constant values of the resonator at two resonance modes.

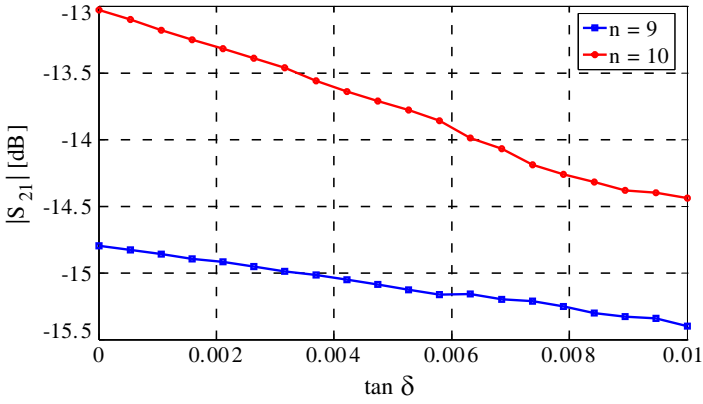

Figure 15. Simulated values of $|S_{21}|$ against different loss tangent values.

5. CONCLUSIONS

A new solution for broadband characterization of dielectric materials, in both liquid and solid states, has been introduced. The proposed WGM sensor has proven to be highly sensitive to small variations within the dielectric properties of the MUT. It has been successfully utilized in characterizing different material samples with the dielectric constant ranging from 2.08 (Teflon) up to 80 (water) in different forms. The MUT is placed on top of the resonator and from the variation of the resonance frequency and Q-factor, the dielectric constant and loss tangent, respectively, have been extracted. The validity of employing resonant perturbation method along with the proposed dielectric resonator has been justified through full-wave simulations and measurements. The sensitivity of the resonator has been also examined to show that the resonator is sensitive to any slight change in dielectric constant and loss tangent. Such results can be promising in various material characterization applications that require precise testing techniques. It can be additionally used to examine human blood and urine for medical purposes.

ACKNOWLEDGMENT

The authors wish to thank Dr. Suren Gigoyan, from the National Academy of Science, Armenia, for his fruitful collaboration in this research work. They also extend their thanks to Mr. Reiner Teuchner, WESGO GmbH, Germany, for providing the Alumina ceramics.

REFERENCES

1. Baker-Jarvis, J., R. G. Geyer, J. H. Grosvenor, Jr., M. D. Janezic, C. A. Jones, B. Riddle, C. M. Weil, and J. Krupka, "Dielectric characterization of low-loss materials: A comparison of techniques," *IEEE Trans. on Dielectrics and Electrical Insulation*, Vol. 5, No. 4, 571–577, Aug. 1998.
2. Williams, T., M. A. Stuchly, and P. Saville, "Modified transmission-reflection method for measuring constitutive parameters of thin flexible high-loss materials," *IEEE Trans. on Microwave Theory and Tech.*, Vol. 51, No. 5, 1560–1566, May 2003.
3. Ocera, A., M. Dionigi, E. Fratticcioli, and R. Sorrentino, "A novel technique for complex permittivity measurement based on a planar four-port device," *IEEE Trans. on Microwave Theory and Tech.*, Vol. 54, No. 6, 2568–2575, Jun. 2006.
4. Kheir, M. S., H. F. Hammad, and A. Omar, "Measurement of the dielectric constant of liquids using a hybrid cavity-ring resonator," *PIERS Proceedings*, 566–569, Cambridge, USA, Jul. 2008.
5. Chen, L. F., C. K. Ong, C. P. Neo, V. V. Varadan, and V. K. Varadan, *Microwave Electronics: Measurement and Material Characterization*, John Wiley & Sons Inc., 2004.
6. Cros, D. and P. Guillon, "Whispering gallery dielectric resonator modes for w-band devices," *IEEE Trans. on Microwave Theory and Tech.*, Vol. 38, No. 11, 1667–1674, Nov. 1990.
7. Jiao, X. H., P. Guillon, L. A. Bermudez, and P. Auxemery, "Whispering-gallery modes of dielectric structures: Applications to millimeter-wave bandstop filters," *IEEE Trans. on Microwave Theory and Tech.*, Vol. 35, No. 12, 1169–1175, Dec. 1987.
8. Neshat, M., S. Gigoyan, D. Saeedkia, and S. Safavi-Naeini, "Travelling-wave whispering gallery resonance sensor in millimetre-wave range," *Electronics Letters*, Vol. 44, No. 17, 1020–1022, Aug. 2008.
9. Krupka, J., K. Derzakowski, A. Abramowicz, M. E. Tobar, and R. G. Geyer, "Use of whispering-gallery modes for complex permittivity determinations of ultra-low-loss dielectric materials," *IEEE Trans. on Microwave Theory and Tech.*, Vol. 47, No. 6, 752–759, Jun. 1999.
10. Krupka, J., D. Mouneyrac, J. G. Hartnett, and M. E. Tobar, "Use of whispering-gallery modes and quasi-TE_{0np} modes for broadband characterization of bulk gallium arsenide and gallium phosphide samples," *IEEE Trans. on Microwave Theory and Tech.*, Vol. 56, No. 5, 1201–1206, May 2008.

11. Shaforosat, E. N., N. Klein, S. A. Vitusevich, A. Offenhausser, and A. A. Barannik, "Nanoliter liquid characterization by open whispering-gallery mode dielectric resonator at millimeter wave frequencies," *Journal of Applied Physics*, Vol. 104, No. 7, 1–7, Oct. 2008.
12. Shaforosat, E. N., N. Klein, S. A. Vitusevich, A. A. Barannik, and N. T. Cherpak, "High sensitivity microwave characterization of organic molecule solutions of nanoliter volume," *Applied Physics Letters*, Vol. 94, No. 11, 1–3, Mar. 2009.
13. Kheir, M. S., H. F. Hammad, and A. Omar, "Non-destructive broadband material characterization over the K-band using whispering-gallery-mode resonators," *Proceedings of the 27th Conference on Precision Electromagnetic Measurements (CPEM2010)*, 285–286, Daejeon, Korea, Jun. 2010.
14. Chen, L., C. K. Ong, and B. T. G. Tan, "Amendment of cavity perturbation method for permittivity measurement of extremely low-loss dielectrics," *IEEE Trans. on Instrumentation and Measurement*, Vol. 48, No. 6, 1031–1037, Dec. 1999.
15. Kraszewski, A. W. and S. O. Nelson, "Observations on resonant cavity perturbation by dielectric objects," *IEEE Trans. on Microwave Theory and Tech.*, Vol. 40, No. 1, 151–155, Jan. 1992.
16. Khanna, A. and Y. Garault, "Determination of loaded, unloaded, and external quality factors of a dielectric resonator coupled to a microstrip line," *IEEE Trans. on Microwave Theory and Tech.*, Vol. 31, No. 3, 261–264, Mar. 1983.
17. Kajfez, D. and P. Guillon, *Dielectric Resonators*, Artech House, Norwood, MA, 1986.
18. Pozar, D. M., *Microwave Engineering*, 2nd Edition, John Wiley & Sons Inc., 1998.
19. CST Microwave Studio, 2009, http://www.cst.com.
20. Wilkes, C. E., C. A. Daniels, and J. W. Summers, *PVC Handbook*, Hanser Publications, 2005.
21. Cuming Microwave Corp., http://www.cumingmw.com.
22. Kheir, M. S., H. F. Hammad, and A. Omar, "Graphical representation and evaluation of attenuation and coupling parameters of whispering-gallery-mode resonators," *IEEE Trans. on Instrumentation and Measurement*, Vol. 60, No. 8, 2942–2950, Aug. 2011.